

Critical Role for Cytosolic Group IVA Phospholipase A₂ in Early Adipocyte Differentiation and Obesity

Lucía Peña,^{1,2} Clara Meana,^{1,2} Alma M. Astudillo,^{1,2} Gema Lordén,^{1,2} Martín Valdearcos,^{1,2} Hiroyasu Sato,³ Makoto Murakami,^{3,4} Jesús Balsinde,^{1,2} and María A. Balboa^{1,2}

¹*Instituto de Biología y Genética Molecular, Consejo Superior de Investigaciones Científicas (CSIC), Universidad de Valladolid, 47003 Valladolid, Spain*

²*Centro de Investigación Biomédica en Red de Diabetes y Enfermedades Metabólicas Asociadas (CIBERDEM), 28029 Madrid, Spain*

³*Lipid Metabolism Project, Tokyo Metropolitan Institute of Medical Science, 2-1-6 Kamikitazawa, Setagaya-ku, Tokyo 156-8506, Japan*

⁴AMED-CREST, Japan Agency for Medical Research and Development, Tokyo 100-0004, Japan

RUNNING TITLE – cPLA₂α is involved in adipogenesis

To whom correspondence should be addressed: University of Valladolid School of Medicine, C/ Sanz y Forés 3, 47010 Valladolid, Spain. Phone, 34-983-184-833; FAX, 34-983-184-800; E-mail: mbalboa@ibgm.uva.es

Keywords: Phospholipase A₂, Adipogenesis, Adipocyte, Obesity, Arachidonic Acid.

Highlights

- Cytosolic group IVA PLA₂α is a key enzyme in arachidonic acid mobilization
- Reduced cytosolic group IVA PLA₂α levels decrease adipocyte differentiation *in vitro* and *in vivo*
- Pretreatment of preadipocytes with arachidonic acid restores adipogenesis
- Cytosolic Group IV PLA₂α has a key role in adipogenesis

ABSTRACT

Adipogenesis is the process of differentiation of immature mesenchymal stem cells into adipocytes. Elucidation of the mechanisms that regulate adipocyte differentiation is key for the development of novel therapies for the control of obesity and related comorbidities. Cytosolic group IVA phospholipase A₂ (cPLA₂α) is the pivotal enzyme in receptor-mediated arachidonic acid (AA) mobilization and attendant eicosanoid production. Using primary multipotent cells and cell lines predetermined to become adipocytes, we show here that cPLA₂α displays a proadipogenic function that occurs very early in the adipogenic process. Interestingly, cPLA₂α levels decrease during adipogenesis, but cPLA₂α-deficient preadipocytes exhibit a reduced capacity to differentiate into adipocytes, which affects early and terminal adipogenic transcription factors. Additionally, the absence of the phospholipase alters proliferation and cell-cycle progression that takes place during adipogenesis. Preconditioning of preadipocytes with AA increases the adipogenic capacity of these cells. Moreover, animals deficient in cPLA₂α show resistance to obesity when fed a high fat diet that parallels changes in the expression of adipogenic transcription factors of the adipose tissue. Collectively, these results show that preadipocyte cPLA₂α activation is a hitherto unrecognized factor for adipogenesis *in vitro* and *in vivo*.

INTRODUCTION

Obesity is a very significant health concern worldwide. Although obesity cannot be considered a disease by itself, it is strongly associated with the onset of insulin resistance, type II diabetes and cardiovascular disease (1). All of these reduce life expectancy and quality, produce early death and collapse healthcare systems. Thus, investigating the mechanisms that support the development of obesity is important for the future discovery of treatments that prevent its occurrence and/or that of its associated disorders.

The expansion of adipose tissue in obesity is caused by an increase in adipocyte number (hyperplasia or adipogenesis) and/or adipocyte size (hypertrophy) (2). Studies in humans suggest that adipose mass in adulthood is determined by the tight regulation of the number of adipocytes (3). Adipogenesis is the complex process through which multipotent mesenchymal precursors commit to the adipocyte lineage and eventually mature into new adipocytes (2, 4).

Different models of *in vitro* adipocyte differentiation, including 3T3-L1 and cultured embryonic fibroblasts from mice have provided useful information to help unravel the cascade of events that take place during adipogenesis (5). Under *in vitro* conditions, adipogenesis requires a period of growth arrest by contact inhibition that ends by treatment with adipogenic factors which promote preadipocytes to re-enter the cell cycle and undergo one or two rounds of mitotic clonal expansion (MCE). Later, cells become permanently growth-arrested and undergo terminal adipocyte differentiation (6-8). The morphological and genetic changes that occur during the process of adipogenic differentiation are regulated by a cascade of transcription factors. After adipogenic induction, cells immediately and transiently express C/EBP β and C/EBP δ , implicated in the expression of C/EBP α , PPAR γ and SREBP-1c. C/EBP α and PPAR γ help each other to maintain their elevated expression throughout the life of the adipocyte and activate the expression of most genes that confer and support the adipocyte phenotype, such as FABP4/aP2, GLUT4 and PLIN2/Adipophilin (9-11). *In vivo* models of adipogenesis include the study of adipose tissue enlargement that follows high fat diet (HFD) (1).

cPLA₂α is one of the most studied members of the PLA₂ superfamily of enzymes, whose common feature is to hydrolyze the fatty acid present in the *sn*-2 position of glycerophospholipids (12, 13). cPLA₂α is widely expressed in mammalian cells, and is the only PLA₂ that shows preference for arachidonic acid (AA)-containing phospholipids as substrates (14). During cellular stimulation its activity is regulated by phosphorylation and intracellular Ca²⁺ concentrations (15). A recent unexpected finding among the many functions attributed to cPLA₂α is that it is necessary for the biogenesis of lipid droplets in various types of cells (16-19). Adipocytes, also known as fat cells, are the cells where lipid droplets have a most prominent role because of their primary fat-storage function. In this regard, although mice lacking cPLA₂α and fed a HFD have been described to exhibit smaller epididymal fat pads and

adipocytes (20), virtually nothing is known about an involvement of cPLA₂α in adipose tissue function or even in the adipogenic process *per se*.

Using multipotent adipose-derived stem cells (ASCs), mouse embryonic fibroblast (MEFs) and cell lines, we identify cPLA₂α as an early key factor for adipocyte differentiation *in vitro*. Furthermore, using cPLA₂α KO animals we also reveal a role for this enzyme during high fat diet (HFD)-induced obesity.

EXPERIMENTAL PROCEDURES

Reagents- Antibodies against β-actin (A5441) were obtained from Sigma-Aldrich (St. Louis, MO, USA). Antibodies against PPARγ (07-466) and FABP4/aP2 (AB3515) were purchased from Merck Millipore Corp. (Billerica, MA, USA). Antibodies against C/EBPα (2295), C/EBPβ (3087), cPLA₂α (2832) and P(Ser505)-cPLA₂α (2831) were obtained from Cell Signaling Technology (Barcelona, Spain). Antibodies against Cdk2 (643901) and Cyclin A (644001) were from BioLegend (San Diego, CA, USA). Antibodies against the nuclear matrix protein p84 (ab487) were from Abcam (Cambridge, UK) and against p115 (612260) were from BD Biosciences (Franklin Lakes, NJ, USA).

Cell culture and differentiation- 3T3-L1 preadipocytes (ATCC CL-173) were maintained in Dulbecco's modified Eagle's medium (DMEM) (Thermo Fisher Scientific Inc., Waltham, MA, USA) containing 10% neonatal calf serum (Thermo Fisher Scientific Inc.) plus 2 mM L-glutamine, 100 U/ml penicillin, 100 µg/ml streptomycin and 25 mM HEPES in a humidified incubator with 5% CO₂. Two days after confluence (differentiation day 0) medium was replaced with DMEM containing 5 µg/ml insulin, 0.5 mM IBMX, 0.25 µM dexamethasone and 10% fetal bovine serum (FBS) (Thermo Fisher Scientific Inc.) (adipogenic differentiation medium 1, ADM1). Two days later, medium was replaced with DMEM containing 5 µg/ml insulin and 10% FBS (ADM2). After three days cells were maintained in medium containing 10 % FBS (adipocyte culture medium).

NIH/3T3 (ATCC CRL-1658) were maintained DMEM containing 10% FBS plus 2 mM L-glutamine, 100 U/ml penicillin, 100 µg/ml streptomycin and 25 mM HEPES, and primary MEFs from 14.5-day mouse embryos were maintained DMEM F-12 containing 10% FBS plus 100 U/ml penicillin and 100 µg/ml streptomycin.

Cells were differentiated according to the protocol described for 3T3-L1 cells, but ADM2 and adipocyte culture medium were supplemented with 10 µM of pioglitazone. Also, the concentration of insulin used for MEFs was 10 µg/ml.

Adipocytes and their precursor cells (ASCs) from murine Swiss epididymal white adipose tissue were isolated by collagenase digestion, as previously described (21). Cells from the stromal-vascular

fraction were cultured on tissue culture plates and were maintained in DMEM F-12 containing 10% FBS plus 100 U/ml penicillin and 100 µg/ml streptomycin in a humidified incubator with 5% CO₂. Cells attaching to the plates constitute ASCs, which were trypsinized and cryopreserved or reseeded. ASCs were differentiated two days after confluence by adding medium containing 10 µg/ml insulin, 0.5 mM IBMX, 1 µM dexamethasone and 200 µM indomethacin. The medium was changed every 3 days and fully differentiated cells were analyzed after 9 days of culture.

Animals- cPLA₂α^{-/-} (*Pla2g4a*^{-/-}) mice and wild type littermates were backcrossed onto the C57BL/6 mice (Japan SLC) for more than 12 generations (22). Animals were kept at 23 °C free of pathogens in a 12-h light-dark cycle without restrictions for water or food consumption. At 8 weeks of age, females were changed to a HFD with 32% of crude fat (HFD 32; CLEA Japan) for 16 weeks (23). All procedures were performed in accordance with approvals by the Institutional Animal Care and Use Committees of Tokyo Metropolitan Institute of Medical Science, Showa University, Japan.

MTT assay- Cell viability was assessed by using a 3-(4,5-dimethylthiazol-2-yl)-2,5-diphenyltetrazolium-bromide (MTT) assay (Sigma-Aldrich). This reagent is reduced by living cells to form an insoluble blue formazan product that can be quantified by absorbance at 570 nm. Cells were treated with 0.5 mg/ml MTT and incubated for 4 h in a CO₂ incubator. Then, cell supernatants were aspirated, cells were treated with isopropanol 100% for 10 min and formazan production was quantified using VersaMax Tunable Microplate Reader (Molecular Devices, Sunnyvale, USA).

Flow cytometry analyses- Cells were trypsinized and collected by centrifugation, washed with PBS, and then fixed in 70% (v/v) cold methanol. Fixed cells were washed with PBS and stained with 50 µg/ml propidium iodide (PI) (Sigma-Aldrich) in the presence of 200 µg/ml RNase A (Sigma-Aldrich) in PBS in the dark for 1 hour. Labeled cells were analyzed using a flow cytometry system Gallios™ (Beckman Coulter, Barcelona, Spain), and data were analyzed using the Kaluza™ software.

Immunoblot- Cells were lysed with 20 mM Tris-HCl (pH 7.4), containing 150 mM NaCl, 0.5% Triton X-100, 1mM Na₃VO₄, 1 mM NaF, 1 mM PMSF (Sigma-Aldrich) and a protease inhibitor cocktail (Sigma-Aldrich) at 4 °C. Homogenates were then clarified by centrifugation at 16,000 x g for 10 min and supernatants used for further analysis.

Extraction of cytoplasmic and nuclear proteins was performed by suspending the cells in 10 mM Tris-HCl (pH 7.5) containing 10 mM NaCl, 3 mM MgCl₂, 100 µM EGTA, 100 µM Na₃VO₄, 1 mM PMSF, a protease inhibitor cocktail (Sigma-Aldrich), 0.5 mM dithiothreitol (Sigma-Aldrich) and 0.05% NP-40 (Merck Millipore Corp.). The cytoplasmic fraction was then clarified by centrifugation at 8000 x g for 2 min. The pellet containing the nuclei was lysed with 20 mM HEPES (pH 7.9), containing 420 mM NaCl, 1.5 mM MgCl₂, 100 µM EDTA, 100 µM Na₃VO₄, 25% glycerol, 1 mM PMSF and a protease

inhibitor cocktail. The nuclear fraction was then clarified by centrifugation at 16000 x g for 10 min and supernatants used for further analysis.

Protein from the supernatants was quantified by the BCA protein assay kit (Thermo Fisher Scientific Inc.) and 50 µg of protein was separated by standard 10-15% SDS-PAGE, transferred to polyvinylidene difluoride membranes (Merck Millipore Corp.) and analyzed by immunoblot using specific antibodies. Detection of immunoreactive bands was conducted by chemiluminescence (Thermo Fisher Scientific Inc.) using a Bio-Rad VersaDoc 5000 system. Digital images were analyzed for quantitative band densitometry at different time exposures within the linear response defined by Quantity One software (Version 4.5.2; Bio-Rad).

Oil Red staining- Differentiated adipocytes were washed with PBS and fixed with 10% formaldehyde in PBS for 1 h, rinsed with 60% isopropanol, and stained with an Oil Red O (Sigma-Aldrich) solution (0.21% Oil Red O in 60% isopropanol) for 10 min. After a final wash with H₂O, digital images of stained plates were taken using a Nikon inverted optical microscope equipped with a Nikon camera. Quantification of cellular lipid accumulation was achieved by extracting Oil Red O from cells with 100% isopropanol for 10 min and measurement of the absorbance at 500 nm using VersaMax Tunable Microplate Reader (Molecular Devices, Sunnyvale, CA, USA) .

RNA interference (siRNA)- To decrease cPLA₂α expression in cells, double strand siRNA oligonucleotides, against mouse cPLA₂α were used (MWG Biotech, Ebersberg, Germany) (sequence, 5'-AGCACAUUCGUGAGUAAUGAUU-3') (24). For knockdown, cells were transfected at 90% confluency with control, nonspecific siRNA, or cPLA₂α siRNA at 40 nM in Opti-MEM® medium (Thermo Fisher Scientific Inc.) using Lipofectamine™ RNAiMAX (Thermo Fisher Scientific Inc.), according to the manufacturer's protocol. The next day, culture medium was replaced with fresh medium and the cells were incubated for additional 24 h. Knockdown of cPLA₂α was verified by immunoblot using specific antibodies.

RNA isolation and quantification- RNA was extracted using TRIzol® reagent method (Thermo Fisher Scientific Inc.). First strand cDNA was synthesized from 2 µg of total RNA using the RETROscript® Kit Reverse Transcription for RT-PCR (Thermo Fisher Scientific Inc.) and random primers. The cDNA was amplified by real time qPCR using the KAPA SYBR® FAST qPCR Master Mix Optimized for LightCycler® 480 (Roche Applied Science, Indianapolis, IN, USA) and specific primers for each gene. Sequences of the primers used are stated in Table I. The relative mRNA abundance for a given gene was calculated using the 2^{-ΔΔC_T} method, using cyclophilin B as the internal standard (25).

Immunocytochemistry- Cells were seeded in coverslips and fixed with 4% paraformaldehyde in PBS containing 2% sucrose for 20 min. Cells were then permeabilized with 0.1% Triton X-100 for 2 min, washed with PBS, and blocked with 5% BSA in PBS for 30 min. p115 immunostaining was performed by

incubating fixed cells with an IgG polyclonal Ab at 1:100 dilution for 1 h followed by a goat anti-IgG-Alexa 594 at 1:200. DAPI (Sigma-Aldrich) stainings were carried out. Cells were then mounted with an antifade solution. Fluorescence was monitored by confocal microscopy using a confocal Leica (Mannheim, Germany) TCS SP5X microscope equipped with a Supercontinuum laser. The objective was HC PL APO 63x, 1.4 numerical aperture, oil immersion. The fluorescence from EGFP was monitored at 485 nm, from Oil Red O and Alexa 594 at 588 nm, and fluorescence from DAPI was monitored at 405 nm using a blue laser diode.

EGFP-cPLA₂α transfection- The plasmid EGFP-cPLA₂α encoding the human cPLA₂α fused to EGFP in its N-terminus was transfected in preadipocytes 3T3-L1 using Lipofectamine™ LTX and PLUS™ (Thermo Fisher Scientific Inc.) reagents following the manufacturer's instructions (26). Adipocytes 3T3-L1 were transfected with 3 µg of plasmid by electroporation using a Gene Pulse Xcell (Bio-Rad laboratories, Hercules, CA, USA).

AA release assay- Evaluation of AA release was performed as previously described (27). In brief, the cells were labeled with 0.5 µCi/ml of [5,6,8,9,11,12,14,15-³H]AA (Sigma-Aldrich) for 20 h. Cells were then washed, treated with the differentiation cocktail and supernatants were removed for radioactivity quantification. Cell monolayers were overlaid with ice-cold PBS containing 0.05% Triton X-100 and scraped. Radioactivity was quantified by liquid scintillation counting in supernatants and homogenates, and AA release was referred to total radioactivity for each condition.

Lipid analysis- Lipids from mice gonadal adipose tissue were extracted using the method described by Folch et al. (28). Lipid classes were separated by thin layer chromatography and their composition in fatty acids were analyzed by GC/MS as previously described (18, 29).

Histology and adipocyte quantification- Samples of gonadal adipose tissue were fixed in paraformaldehyde, embedded in paraffin, cut, and stained with hematoxylin and eosin (23). From micrographs pictures, the area of randomly selected adipocytes was measured using the ImageJ image analysis software. After calculating the frequency distribution for the areas, adipocyte number in WAT was calculated as previously described (30).

Statistics- All values are given as means ± SEM. Differences between two groups were assessed by using the unpaired Student's t-test. A *p* value < 0.05 was considered statistically significant.

RESULTS

cPLA₂α decreases its expression levels during adipogenesis- We started this work by looking for possible differences in the expression levels of PLA₂ family members between stromal-vascular fraction (SVF) cells, which include adipocyte precursors and adipocytes isolated from white adipose tissue of

mice. We noted significant increases in mRNA levels of some PLA₂s, namely groups IIE, VIA, VIB, VID, VIE and XVI (Figure 1A), but a very specific change was the disappearance of the mRNA for group IVA PLA₂ (cPLA₂α). No other PLA₂ gene decreased under these conditions. The expression levels of the preadipocyte specific factor, *Pref1* and the adipocyte markers *Pparg*, *Fabp4*, and *Lipin1* were also evaluated to confirm the nature of the cells under study (Figure 1B). We also assayed cPLA₂α protein levels by immunoblot in SVF cells, adipocytes and total adipose tissue, finding that SVF cells have the highest expression and that adipocytes have very low levels of the enzyme (Figure 1C). We next investigated if during the differentiation process to adipocytes, ASCs decrease their cPLA₂α levels. To this end, isolated ASCs were differentiated *in vitro* and by analyzing mRNA and protein levels for cPLA₂α, we confirmed that cPLA₂α actually decreases during adipogenesis (Figures 1D-F). When adipocyte differentiation was examined using the 3T3-L1 preadipocytic cell line, essentially the same results were observed regarding PLA₂ family expression pattern and cPLA₂α expression levels (Figure 2).

Reducing the levels of cPLA₂α in preadipocytes decreases adipogenesis– We next examined the impact of cPLA₂α on adipogenesis by using multipotent MEFs from cPLA₂α^{-/-} mice, where the expression of the enzyme is completely suppressed (Figure 3). Elimination of cPLA₂α expression completely abolished the capacity of MEFs to become adipocytes (Figures 3), and a drastic reduction in neutral lipid storage (close to 90% reduction, measured by Oil Red O staining) was detected after 8 days of adipogenic induction. Also, the expression of adipocyte specific markers (*Fabp4/aP2*, GLUT4, *Plin2/Adipophilin*) and transcription factors (PPAR_γ, C/EBP_α, SREBP-1c) was abrogated at both protein and mRNA level (Figures 3B and C).

Multipotent cells such as the NIH/3T3 cell line and the preadipocytic cell line 3T3-L1, were also used in these studies, using siRNA technology to decrease cPLA₂α (Figures 3D-E, and 4). The same behavior as described above was observed in the absence of cPLA₂α. Collectively, these data demonstrate that adipocyte precursors need cPLA₂α to completely differentiate into adipocytes.

cPLA₂α is activated early after adipogenic induction– We next sought to analyze the time period at which cPLA₂α acts within the differentiation process. As a direct measure of cPLA₂α activation, we analyzed AA release from 3T3-L1 cells treated with the differentiation cocktail. The results showed a very sharp release of the fatty acid early on, reaching a plateau 3-4 h after induction (Figure 5A). Reduction of cPLA₂α expression significantly affected the release of AA, confirming the importance of the enzyme in the process (Figure 5B). The time-course of AA release paralleled the phosphorylation of the enzyme in Ser⁵⁰⁵, which is a hallmark of activation (Figure 5C). We found that FBS caused the same level of phosphorylation as the complete ADM1 (Figure 5D). By analyzing the localization of cPLA₂α during the differentiation of 3T3-L1 cells, we found that the enzyme exhibits a cytosolic diffuse

localization in preadipocytes, while it localizes mainly in the Golgi in fully differentiated adipocytes (colocalization with the Golgi specific protein p115) (Figures 5E and F). Analogous localization of cPLA₂α in the absence of high intracellular Ca²⁺ levels has been associated with inactivation of the enzyme (31). Taken together, these data suggest that cPLA₂α acts early during adipocyte differentiation.

cPLA₂α affects several early processes after adipogenic induction—Next, we investigated which of the early events of adipocyte differentiation process were affected by abrogation of cPLA₂α expression. Mitotic clonal expansion is a well documented event that occurs very early during the differentiation process and is required for adipocyte differentiation (8). We found that 3T3-L1 cells treated with siRNA against cPLA₂α experienced diminished proliferation levels as compared to control cells for the first 2 days after adipogenic induction (Figure 6A). Cell cycle analyses by flow cytometry demonstrated that, while the majority of control cells were at the G₂/M phase of the cell cycle after 24 h of adipogenic induction, cells with reduced levels of cPLA₂α underwent a delay that retained many of them in the first phases of the cell cycle (Figure 6B and C). In agreement with these findings, we found that key factors for cell cycle progression such as cyclin A or Cdk2 had a delayed expression in cells exhibiting reduced levels of cPLA₂α (Figure 6D).

Expression of very early transcription factors like C/EBPβ was also delayed in cPLA₂α-deficient cells (Figure 6E). As a consequence of it, the expression of transcription factors that are controlled by C/EBPβ, like C/EBPα and SREBP-1c had a reduced expression that could already be noticed at day 2 after adipogenic induction (Figure 4F). These data indicate that cPLA₂α is important for early adipogenic events.

Exogenous AA enhances adipogenesis during the cell-contact inhibition state – All the cell systems used in this work show reduced expression levels of cPLA₂α at the time of adipogenic induction. Thus we reasoned that at least part of the proadipogenic function of cPLA₂α could be exerted in the preadipocyte when its expression levels are higher. To obtain experimental support for this suggestion, we treated preadipocytes 3T3-L1 with exogenous AA 2 days prior to induction of adipogenesis, i.e. when proliferation of cells is inhibited by cell contact (confluence phase). As shown in Figure 7, AA accelerated the expression of the cell cycle-related proteins cyclin A and Cdk2. As a consequence, the AA-treated cells entered earlier into the G₂/M phase (Figure 7B and C) and proliferated more than control cells (Figure 7A). Moreover, AA increased the accumulation of neutral lipids in mature adipocytes (Oil Red O staining, Figure 8A) as well as the expression of adipocyte markers (*Fabp4/aP2*, GLUT4, *Plin2/Adipophilin*) (Figure 8B and C), and also the expression of early (C/EBPβ, Figure 7E) and late (PPARγ, C/EBPα and SREBP-1c, Figure 8B and C) adipocyte transcription factors. We also observed a feedback loop between AA and cPLA₂α, because AA-treated preadipocytes increased their content of the

enzyme (Figure 8D), an effect that continued during the first two days of adipogenic induction. By treating the cells with the cyclooxygenase inhibitor indomethacin, we found that only part of the effects of AA on adipogenesis was due to prostaglandin generation (Figure 8E). Overall, these data demonstrate that treatment of preadipocytes with AA during the cell-contact inhibition phase increases adipogenesis.

cPLA₂α KO mice are protected against HFD induced obesity—We next sought to determine the relevance of cPLA₂α during HFD induced obesity in mice. To this end we fed cPLA₂α^{+/+} and cPLA₂α^{-/-} mice with a HFD for 16 weeks. We observed that cPLA₂α^{-/-} animals gained less weight than cPLA₂α^{+/+} animals (Figures 9B-C). Also, white adipose tissue (WAT) but not brown adipose tissue (BAT) weight was affected, suggesting a role for cPLA₂α in the first tissue but not in the second one (Figure 9D). Importantly, lean mass was not significantly affected by the absence of cPLA₂α (Figure 9E). Analysis of the frequency distribution of adipocyte cell surface area demonstrated a significant reduction in the frequency of bigger cells and an enrichment in smaller cells in the adipose tissue of cPLA₂α^{-/-} mice, suggesting a reduced lipid accumulation, or hypertrophy, in these animals (Figure 9F and G). Moreover, cPLA₂α^{-/-} animals had a decreased number of adipocytes in their WAT pads (Figure 9H). The phenotype correlated with a reduced accumulation of triglycerides and cholesteryl esters, and a significant increase in phospholipids in the adipose tissue of cPLA₂α^{-/-} animals (Figure 9I). Analysis of adipocyte markers and transcription factors showed a significantly lower mRNA level for C/EBPβ, SREBP-1c and Adipophilin, and a significant increase in the mRNA for the preadipocytic marker Pref-1 (Figure 9J).

Together, the data indicate that cPLA₂α participates in adipogenesis (hyperplasia), and lipid accumulation (hypertrophy) that occur in the adipose tissue during feeding a HFD.

DISCUSSION

The present study shows that cPLA₂α is required for adipogenesis of multipotent cells such as MEFs and the cell line NIH/3T3, and the committed preadipocytic cell line 3T3-L1. These data provide support for a key role for cPLA₂α in *in vitro* differentiation. Furthermore, animals deficient in cPLA₂α that are subjected to a HFD show a reduced capacity to increase body weight and fat mass, confirming the important role for the enzyme during the enlargement of the adipose tissue in these circumstances.

cPLA₂α is a unique enzyme within the PLA₂ superfamily in many respects. For instance, cPLA₂α is the only PLA₂ that shows marked preference for AA chains within glycerophospholipids; it translocates to intracellular membranes in response to an intracellular Ca²⁺ rise, and is phosphorylated by MAPKs during activation (12,15,32,33). It has recently been found that up-regulation of enzymes related to eicosanoid production such as PLA₂ influence the type and quantity of eicosanoids regulating adipose

tissue differentiation (34). The present study adds an interesting unique feature for the AA-releasing cPLA₂α, as playing a fundamental role at the beginning of adipocyte differentiation. In most cells, cPLA₂α expression levels are generally stable, its activity being tightly regulated by events triggered after receptor stimulation (12,13,15,26,35,36). The finding that during adipogenesis, cPLA₂α levels fall sharply is striking. Cell treatment with glucocorticoids has previously been related with decreases in cPLA₂α expression levels by affecting *de novo* mRNA synthesis (37). During adipocytic differentiation *in vitro*, the glucocorticoid dexamethasone, which is present in the differentiation cocktail, may account for the reduction in enzyme levels. Interestingly, we have also detected an important reduction in the levels of cPLA₂α mRNA and protein between SVF cells and adipocytes from mouse adipose tissue, probably reflecting that the natural adipocyte differentiation process also proceeds with a reduction of the enzyme. Whether this effect is related with glucocorticoid levels generated during adipogenesis *in vivo* remains to be elucidated.

Along our experimentation we have also found that pretreatment of preadipocytes with AA increases the level of cPLA₂α. This feedback loop was unexpected, inasmuch as AA is the downstream product of the enzyme. Thus, it is possible the differentiating effects that AA exerts on preadipocytes may be due to increased cPLA₂α expression in these cells. The molecular mechanism governing this process remains to be elucidated. cPLA₂α has an AP-1 binding site in its promoter that can mediate upregulation of the enzyme (38).

During adipogenesis cPLA₂α sustains the early expression of several key factors such as the transcription factor C/EBPβ, and cell cycle-related proteins. C/EBPβ is necessary for the expression of the terminal adipogenic transcription factors C/EBPα and PPARγ, and the development of functions that characterize mature adipocytes, such as lipogenesis and lipid accumulation (9,10). The expression of C/EBPβ and cell cycle-related proteins such as cyclin A is related with increases in cAMP, activation of PKA and phosphorylation of the transcription factor CREB (39, 40). In this regard, it has been described that AA can substitute for IBMX, the molecule present in the adipogenic cocktail that increases cAMP levels during the induction of adipocyte differentiation (41). However, if AA and IBMX are added together to preadipocytes, there is a reduction of adipogenesis that can be restored with PKA inhibitors (41). These effects suggest that under these conditions the levels of cAMP are very high and produce detrimental effects on adipogenesis. However, in a natural adipogenic process where IBMX is not present and cAMP levels are not high, cPLA₂α could contribute to the generation of cAMP and the propagation of downstream effects. For example, recent evidence has been provided that in addition of prostacyclin and PGE₂, other downstream products of cPLA₂α such as leukotriene E₄ may act to elevate the

intracellular levels of cAMP (42). Consistent with this is our finding that pretreatment of preadipocytes with AA during two days without IBMX promotes adipogenesis.

Our *in vivo* studies show that cPLA₂α plays a role in regulating the expression of C/EBPβ and SREBP-1c during HFD. SREBP-1c is a target for C/EBPβ during adipogenesis, and thus their expression levels are connected (43). The function of SREBP-1c in adipogenesis is to regulate the expression of genes of lipid metabolism, and the production of endogenous PPARγ ligands (11,44). This suggests that, although the expression of PPARγ is not affected by cPLA₂α in animals on a HFD, its activation level could be determined by the endogenous ligands produced by SREBP-1c, impacting in this way on the differentiation process. Thus, by regulating the levels of C/EBPβ and SREBP-1c, cPLA₂α determines the levels of both adipogenesis and adipocyte hypertrophy *in vivo*.

Not only ASCs exhibit high levels of cPLA₂α in the adipose tissue, but macrophages also are very rich sources of this enzyme (45). These are cells with a very high capacity to release AA when activated by many different stimuli (46-48). In the adipose tissue, obesity promotes infiltration of macrophages, which may account for up to 60% of all cells in the tissue (49), likely increasing the capacity of the tissue to generate AA from phospholipid stores. There are several effectors produced under these circumstances that may act to increase AA release by the macrophages. For example, palmitic acid produced by aberrant lipolysis in stressed adipocytes could activate TLR4 on the surface of macrophages (46). Also, enhanced production of TNFα during obesity could impact on macrophages to release AA (49). Thus the possibility exists that, in obesity, activated macrophages that are part of the stromal-vascular fraction of cells, and are very proximal to ASCs, release substantial amounts of AA that in a paracrine manner would impact in ASCs increasing adipogenesis of these cells. In support of this view, a very strong correlation between adipocyte size and macrophage number in adipose tissue has been reported (50).

Collectively our data show that cPLA₂α is a positive regulator of adipogenesis. cPLA₂α regulates early adipogenic processes related with the expression of transcription factors and cell cycle progression during the mitotic clonal expansion associated to adipogenesis. Also, in obesity, cPLA₂α is involved in adipose tissue expansion and neutral lipid deposition. Future research should evaluate whether pharmacological inhibition of the enzyme affects obesity and related comorbidities.

Acknowledgments: We thank Montse Duque and Yolanda Noriega for excellent technical assistance. We are grateful to Dr. José Javier García Ramirez (School of Medicine, University of Castilla La Mancha, Albacete, Spain) for providing 3T3-L1 and NIH/3T3 cells, and Dr. Takao Shimizu (Department of Biochemistry and Molecular Biology, the University of Tokyo, Japan) for providing breeding groups of heterozygous cPLA₂α-deficient mice. This work was supported by the Spanish Ministry of Science and Innovation (Grants SAF2010-18831, BFU2010-18826 and SAF2013-48201-R), the Regional Government of Castile and Leon (Grants BIO39/VA04/10, CSI168A12-1 and BIO/VA03/14) and by grants-in aid for Scientific Research from the Ministry of Education, Culture, Sports, Science and Technology of Japan and AMED-CREST from the Japan Agency for Medical Research and Development (MM and HS). L.P. and G.L. were supported by predoctoral fellowships from the Spanish Ministry of Science and Innovation (*Plan de Formación de Personal Investigador* and *Plan de Formación de Profesorado Universitario* programs, respectively). M.V. was supported by a predoctoral fellowship from the Regional Government of Castile and Leon. CIBERDEM is an initiative of *Instituto de Salud Carlos III*.

Conflict of interest: The authors declare that they have no conflicts of interest with the contents of this article.

Author contributions: L.P. acquisition of data, analyses and interpretation of data, manuscript preparation, statistical analyses. C.M. acquisition of data, analyses and interpretation of data. A.A. acquisition of data, analyses and interpretation of data. G.L. acquisition of data, analyses and interpretation of data. M.V. acquisition of data, analyses and interpretation of data. H.S. acquisition of data, analyses and interpretation of data. M.M. analyses and interpretation of data, manuscript preparation. J.B. analyses and interpretation of data, manuscript preparation. M.A.B. study conception, study design, analyses and interpretation of data, and manuscript preparation.

REFERENCES

1. Gregor, M. F., and Hotamisligil, G. S. (2011) Inflammatory mechanisms in obesity. *Annu. Rev. Immunol.* **29**, 415-445
2. Otto, T. C., and Lane, M. D. (2005) Adipose development: from stem cell to adipocyte. *Crit. Rev. Biochem. Mol. Biol.* **40**, 229-242
3. Spalding, K. L., Arner, E., Westermark, P. O., Bernard, S., Buchholz, B. A., Bergmann, O., Blomqvist, L., Hoffstedt, J., Näslund, E., Britton, T., Concha, H., Hassan, M., Rydén, M., Frisén, J., and Arner, P. (2008) Dynamics of fat cell turnover in humans. *Nature* **453**, 783-787
4. Spiegelman, B. M., and Flier, J. S. (1996) Adipogenesis and obesity: rounding out the big picture. *Cell* **87**, 377-389
5. Gregoire, F. M., Smas, C. M., and Sul, H. S. (1998) Understanding adipocyte differentiation. *Physiol. Rev.* **78**, 783-809
6. Richon, V. M., Lyle, R. E., and McGehee, R. E. Jr. (1997) Regulation and expression of retinoblastoma proteins p107 and p130 during 3T3-L1 adipocyte differentiation. *J. Biol. Chem.* **272**, 10117-10124
7. Reichert, M., and Eick, D. (1999) Analysis of cell cycle arrest in adipocyte differentiation. *Oncogene* **18**, 459-466
8. Tang, Q. Q., Otto, T. C., and Lane, M. D. (2003) Mitotic clonal expansion: a synchronous process required for adipogenesis. *Proc. Natl. Acad. Sci. U.S.A.* **100**, 44-49
9. Rosen, E.D. (2002) Molecular mechanisms of adipocyte differentiation. *Ann. Endocrinol. (Paris)* **63**, 79-82
10. Tontonoz, P., and Spiegelman, B. M. (2008) Fat and beyond: the diverse biology of PPAR γ . *Annu. Rev. Biochem.* **77**, 289-312
11. Eberlé, D., Hegarty, B., Bossard, P., Ferré, P., and Fufelle, F. (2004) SREBP transcription factors: master regulators of lipid homeostasis. *Biochimie* **86**, 839-848
12. Dennis, E. A., Cao, J., Hsu, Y. H., Magrioti, V., and Kokotos, G. (2011) Phospholipase A₂ enzymes: physical structure, biological function, disease implication, chemical inhibition, and therapeutic intervention. *Chem. Rev.* **111**, 6130-6185
13. Balsinde, J., Balboa, M. A., Insel, P. A., and Dennis, E. A. (1999) Regulation and inhibition of phospholipase A₂. *Annu. Rev. Pharmacol. Toxicol.* **39**, 175-189
14. Clark, J. D., Lin, L. L., Kriz, R. W., Ramesha, C. S., Sultzman, L. A., Lin, A. Y., Milona, N., and Knopf, J. L. (1991) A novel arachidonic acid-selective cytosolic PLA₂ contains a Ca²⁺-dependent translocation domain with homology to PKC and GAP. *Cell* **65**, 1043-1051
15. Ghosh, M., Tucker, D. E., Burchett, S. A., and Leslie, C. C. (2006) Properties of the Group IV phospholipase A₂ family. *Prog. Lipid. Res.* **45**, 487-510
16. Gubern, A., Casas, J., Barceló-Torns, M., Barneda, D., de la Rosa, X., Masgrau, R., Picatoste, F., Balsinde, J., Balboa, M. A., and Claro, E. (2008) Group IVA phospholipase A₂ is necessary for the biogenesis of lipid droplets. *J. Biol. Chem.* **283**, 27369-27382
17. Gubern, A., Barceló-Torns, M., Barneda, D., López, J. M., Masgrau, R., Picatoste, F., Chalfant, C. E., Balsinde, J., Balboa, M. A., and Claro, E. (2009) JNK and ceramide kinase govern the biogenesis of lipid droplets through activation of group IVA phospholipase A₂. *J. Biol. Chem.* **284**, 32359-32369
18. Guijas, C., Pérez-Chacón, G., Astudillo, A. M., Rubio, J. M., Gil-de-Gómez, L., Balboa, M. A., and Balsinde, J. (2012) Simultaneous activation of p38 and JNK by arachidonic acid stimulates the cytosolic phospholipase A₂-dependent synthesis of lipid droplets in human monocytes. *J. Lipid Res.* **53**, 2343-2354
19. Guijas, C., Rodriguez, J. P., Rubio, J.M., Balboa, M.A., and Balsinde, J. (2014) Phospholipase A₂ regulation of lipid droplet formation. *Biochim. Biophys. Acta* **1841**, 1661-1671

20. Li, H., Yokoyama, N., Yoshida, S., Tsutsumi, K., Hatakeyama, S., Sato, T., Ishihara, K., and Akiba, S. (2009) Alleviation of high-fat diet-induced fatty liver damage in group IVA phospholipase A₂-knockout mice. *PLoS One* **4**, e8089.
21. Rodbell, M. (1964) Metabolism of isolated fat cells. I. Effects of hormones on glucose metabolism and lipolysis. *J. Biol. Chem.* **239**, 375-80
22. Uozumi, N., Kume, K., Nagase, T., Nakatani, N., Ishii, S., Tashiro, F., Komagata, Y., Maki, K., Ikuta, K., Ouchi, Y., Miyazaki, J., and Shimizu, T. (1997) Role of cytosolic phospholipase A₂ in allergic response and parturition. *Nature* **390**, 618-622
23. Sato, H., Taketomi, Y., Ushida, A., Isogai, Y., Kojima, T., Hirabayashi, T., Miki, Y., Yamamoto, K., Nishito, Y., Kobayashi, T., Ikeda, K., Taguchi, R., Hara, S., Ida, S., Miyamoto, Y., Watanabe, M., Baba, H., Miyata, K., Oike, Y., Gelb, M. H., and Murakami, M. (2014) The adipocyte-inducible secreted phospholipases PLA2G5 and PLA2G2E play distinct roles in obesity. *Cell. Metab.* **20** 119-132
24. Pindado, J., Balsinde, J., and Balboa, M. A. (2007) TLR-3-dependent induction of nitric oxide synthase in macrophages via a cytosolic phospholipase A₂/ Cyclooxygenase-2 pathway. *J. Immunol.* **179**, 4821-4828
25. Livak, K.J., and Schmittgen, T. D. (2001) Analysis of relative gene expression data using real-time quantitative PCR and the 2(-Delta Delta C(T)) *Methods* **25**, 402-408
26. Casas, J., Gijón, M. A., Vigo, A. G., Crespo, M. S., Balsinde, J., and Balboa, M. A. (2006) Phosphatidylinositol 4,5-bisphosphate anchors cytosolic group IVA phospholipase A₂ to perinuclear membranes and decreases its calcium requirement for translocation in live cells. *Mol. Biol. Cell* **17**, 155-162
27. Casas, J., Meana, C., Esquinas, E., Valdearcos, M., Pindado, J., Balsinde, J., and Balboa, M. A. (2009) Requirement of JNK-mediated phosphorylation for translocation of group IVA phospholipase A₂ to phagosomes in human macrophages. *J. Immunol.* **183**, 2767-2774
28. Folch, J., Lees, M., and Sloane Stanley, G. H. (1957) A simple method for the isolation and purification of total lipides from animal tissues. *J. Biol. Chem.* **226** 497-509
29. Astudillo, A. M., Pérez-Chacón, G., Balgoma, D., Gil-de-Gómez, L., Ruipérez, V., Guijas, C., Balboa, M. A., and Balsinde, J. (2011) Influence of cellular arachidonic acid levels on phospholipid remodeling and CoA-independent transacylase activity in human monocytes and U937 cells. *Biochim. Biophys. Acta* **1811**, 97-103
30. Jo, J., Gavrilova, O., Pack, S., Jou, W., Mullen, S., Sumner, A. E., Cushman, S. W., and Periwai, V. (2009) Hypertrophy and/or hyperplasia: dynamics of adipose tissue growth. *PLoS Comput. Biol.* **5**, e1000324.
31. Herbert, S. P., Odell, A. F., Ponnambalam, S., and Walker, J. H. (2007) The confluence-dependent interaction of cytosolic phospholipase A₂-alpha with annexin A1 regulates endothelial cell prostaglandin E₂ generation. *J. Biol. Chem.* **282**, 34468-34478
32. Pérez-Chacón, G., Astudillo, A. M., Balgoma, D., Balboa, M. A., and Balsinde, J. (2009) Control of free arachidonic acid levels by phospholipases A₂ and lysophospholipid acyltransferases. *Biochim. Biophys. Acta* **1791**, 1103-1113
33. Astudillo, A. M., Balgoma, D., Balboa, M. A., and Balsinde, J. (2012) Dynamics of arachidonic acid mobilization by inflammatory cells. *Biochim. Biophys. Acta* **1821**: 249-256
34. Polus, A., Kiec-Wilk, B., Razny, U., Gielicz, A., Schmitz, G., and Dembinska-Kiec, A. (2015) Influence of dietary fatty acids on differentiation of human stromal vascular fraction preadipocytes. *Biochim. Biophys. Acta* **1851**, 1146-11455.
35. Pettus, B. J., Bielawska, A., Subramanian, P., Wijesinghe, D. S., Maceyka, M., Leslie, C. C., Evans, J. H., Freiberg, J., Roddy, P., Hannun, Y. A., and Chalfant, C. E. (2004) Ceramide 1-phosphate is a direct activator of cytosolic phospholipase A₂. *J. Biol. Chem.* **279**, 11320-11326

36. Casas, J., Valdearcos, M., Pindado, J., Balsinde, J., and Balboa, M. A. (2010) The cationic cluster of group IVA phospholipase A₂ Lys488/Lys541/Lys543/Lys544) is involved in translocation of the enzyme to phagosomes in human macrophages. *J. Lipid. Res.* **51**, 388-399
37. Dolan-O'keefe, M., and Nick, H. S. (1999) Inhibition of cytoplasmic phospholipase A₂ expression by glucocorticoids in rat intestinal epithelial cells. *Gastroenterology* **116**, 855-864
38. Lee, I.T., Lin, C.C., Cheng, S.E., Hsiao, L.D., Hsiao, Y.C., and Yang, C.M. (2013) TNF- α induces cytosolic phospholipase A₂ expression in human lung epithelial cells via JNK1/2- and p38 MAPK-dependent AP-1 activation. *PLoS One* **8**:e72783.
39. Belmonte, N., Phillips, B. W., Massiera, F., Villageois, P., Wdziekonski, B., Saint-Marc, P., Nichols, J., Aubert, J., Saeki, K., You, A., Narumiya, S., Ailhaud, G., and Dani, C. (2001) Activation of extracellular signal-regulated kinases and CREB/ATF-1 mediate the expression of CCAAT/enhancer binding proteins beta and -delta in preadipocytes. *Mol. Endocrinol.* **15**, 2037-2049
40. Desdouets, C., Matesic, G., Molin, C. A., Foulkes, N.S., Sassone-Corsi, P., Brechot, C., and Sobczak-Thepot, J. (1995) Cell cycle regulation of cyclin A gene expression by the cyclic AMP-responsive transcription factors CREB and CREM. *Mol. Cell. Biol.* **15**, 3301-3309
41. Madsen, L., Pedersen, L. M., Liaset, B., Ma, T., Petersen, R. K., van den Berg, S., Pan, J., Müller-Decker, K., Dülsner, E. D., Kleemann, R., Kooistra, T., Døskeland, S.O., and Kristiansen, K. (2008) cAMP-dependent signaling regulates the adipogenic effect of n-6 polyunsaturated fatty acids. *J. Biol. Chem.* **283**:7196-7205
42. Steinke, J.W., Negri, J., Payne, S.C., and Borish, L. (2014) Biological effects of leukotriene E₄ on eosinophils. *Prostag. Leukot. Essent. Fatty Acids* **91**: 105-110
43. Payne, V. A., Au, W. S., Lowe, C.E., Rahman, S.M., Friedman, J. E., O'Rahilly, S., and Rochford, J. J. (2009) C/EBP transcription factors regulate SREBP1c gene expression during adipogenesis. *Biochem. J.* **425**, 215–223
44. Kim, J.B., Wright, H.M., Wright, M., and Spiegelman, B.M. (1998) ADD1/SREBP1 activates PPAR γ through the production of endogenous ligand. *Proc. Natl. Acad. Sci. U. S. A.* **95**, 4333-4337
45. Leslie, C. C. (1991) Kinetic properties of a high molecular mass arachidonoyl-hydrolyzing phospholipase A₂ that exhibits lysophospholipase activity. *J. Biol. Chem.* **266**, 11366-11371
46. Ruipérez, V., Astudillo, A. M., Balboa, M. A., and Balsinde, J. (2009) Coordinate regulation of Toll-like receptor-mediated arachidonic acid mobilization in macrophages by group IVA and group V phospholipase A₂s. *J. Immunol.* **182**, 3877-3883
47. Astudillo, A. M., Pérez-Chacón, G., Meana, C., Balgoma, D., Pol, A., del Pozo, M. A., Balboa, M. A., and Balsinde, J. (2011) Altered arachidonate distribution in macrophages from caveolin-1 null mice leading to reduced eicosanoid synthesis. *J. Biol. Chem.* **286**, 35299-35307.
48. Gil-de-Gómez, L., Astudillo, A. M., Guijas, C., Magrioti, V., Kokotos, G., Balboa, M. A., and Balsinde, J. (2014) Cytosolic group IVA and calcium-independent group VIA phospholipase A₂s act on distinct phospholipid pools in zymosan-stimulated mouse peritoneal macrophages. *J. Immunol.* **192**: 752-762
49. McPhillips, K., Janssen, W.J., Ghosh, M., Byrne, A., Gardai, S., Remigio, L., Bratton, D. L., Kang, J. L., and Henson, P. (2007) TNF-alpha inhibits macrophage clearance of apoptotic cells via cytosolic phospholipase A₂ and oxidant-dependent mechanisms. *J. Immunol.* **178**, 8117-8126
50. Weisberg, S.P., McCann, D., Desai, M., Rosenbaum, M., Leibel, R. L., and Ferrante, A.W, Jr. (2003) Obesity is associated with macrophage accumulation in adipose tissue. *J. Clin. Invest.* **112**, 1796-1808

FOOTNOTES

The abbreviations used are: ADM, adipogenic differentiation medium; AA, arachidonic acid; cPLA₂α, cytosolic group IVA phospholipase A₂α; MCE, mitotic clonal expansion; ASCs, adipose stem cell ; MEFs, mouse embryonic fibroblast; HFD, high fat diet; MTT; 3-(4,5-dimethylthiazol-2-yl)-2,5-diphenyltetrazolium-bromide.

FIGURE LEGENDS

FIGURE 1. *cPLA₂α expression is reduced during ASCs differentiation.* (A) SVF cells and adipocytes (AD) were isolated from mice adipose tissue and the levels of mRNA of the PLA₂ family genes were analyzed by qPCR. (B) qPCR analysis of adipogenesis related genes in samples shown in A. (C) Homogenates from SVF cells, AD and total adipose tissue were analyzed by immunoblot for cPLA₂α expression. β-Actin was used as loading control. Since AD express low levels of β-Actin, asterisk denotes a nonspecific band that shows similar signal for AD and SVF cells. Lower panel shows the relative quantification of cPLA₂α expression against β-Actin. (D) ASCs were isolated and differentiated *in vitro*. Pictures from day 0 and 9 after differentiation are shown. (E) ASCs mRNA levels for cPLA₂α (*Pla2g4a*) were analyzed by qPCR at different time points during adipogenesis. (F) ASCs homogenates were analyzed for cPLA₂α expression by immunoblot. Relative quantification against β-Actin is shown in the lower panel. Error bars represent the SEM of three independent determinations and statistical significance is indicated * p<0.05, ** p<0.01, *** p<0.001. Experiments are representative of at least three different ones.

FIGURE 2. *cPLA₂α expression decreases during differentiation in 3T3-L1.* (A) qPCR analysis of mRNA levels of PLA₂ family genes in 3T3-L1 cells before and 8 days after adipogenic induction. (B) Pictures of cells treated like in A and stained with Oil Red O are shown. (C) Quantitative analysis of mRNA levels of adipogenesis related genes in samples shown in A. (D) Homogenates from 3T3-L1 cells induced to differentiate for the indicated periods of time were analyzed by immunoblot using specific antibodies against cPLA₂α and β-Actin as a loading control. (E) Cells treated as in D were analyzed by qPCR for quantification of cPLA₂α mRNA levels. In all experiment shown error bars represent the SEM of three independent determinations and statistical significance is indicated * p<0.05, ** p<0.01, *** p<0.001. Experiments are representative of at least three different ones.

FIGURE 3. *cPLA₂α regulates adipogenesis in primary cells.* (A) MEFs from cPLA₂α^{+/+} or cPLA₂α^{-/-} mice were induced to differentiate in adipocytes for 8 days and were stained with Oil Red O. Pictures from cells and culture plates are shown. Right panel shows the quantification of Oil Red O staining. (B) MEFs homogenates from cells treated as in A were analyzed by immunoblot for the expression of the indicated proteins related with adipogenesis. β-Actin or p84 were used as loading controls for total and nuclear proteins. (C) Quantification by qPCR of mRNA levels of the indicated genes from MEFs treated as in A. (D) Confluent NIH-3T3 cells were treated with siRNA control or against cPLA₂α for two days, induced to differentiate in adipocytes for 8 days and stained with Oil Red O. Pictures of cells and culture plates are shown. Right panel shows the quantification of Oil Red O staining. (E) Homogenates from NIH-3T3 cells treated as in D were analyzed by immunoblot for the expression of the indicated proteins related with adipogenesis. Error bars represent the SEM of three independent determinations and statistical significance is indicated * p<0.05, ** p<0.01. The experiments shown are representative of at least three different ones.

FIGURE 4. *cPLA₂α is important for adipogenesis of 3T3-L1 cells.* (A-F) Confluent 3T3-L1 cells were treated with siRNA control or against cPLA₂α for two days, induced to differentiate in adipocytes for 8 days and stained with Oil Red O. Pictures of cells are shown in A. (B) Quantification of differentiated adipocytes from cells analyzed in A. (C) Pictures of cell culture plates are shown. (D) Quantification of Oil Red O staining. (E) Homogenates from cells treated as in A were analyzed by immunoblot for the expression of the indicated proteins related with adipogenesis. (F) Cells treated as in A were analyzed by qPCR for quantification of mRNA levels of the indicated genes. For all the experiments presented error bars represent the SEM of three independent determinations and statistical significance is indicated ** p<0.01. At least three independent experiments were performed.

FIGURE 5. *cPLA₂α acts very early during adipogenesis.* (A) 3T3-L1 labeled with 0.5 μCi [³H]AA cells were induced to differentiate. [³H]AA released to the supernatant was quantified at different time points. (B) 3T3-L1 cells treated with siRNA control or against cPLA₂α were induced to differentiate for 4 h and AA release was analyzed as in A. (C) 3T3-L1 cells were induced to differentiate for the indicated time points and homogenates were analyzed by immunoblot using specific antibodies for cPLA₂α or its Ser⁵⁰⁵ phosphorylated form. Lower panel represents relative quantification of phosphorylated bands. (D) 3T3-L1 cells were treated with ADM1 or with each its components separately, as indicated. Proteins from homogenates were analyzed as in C. (E) 3T3-L1 transfected with the plasmid EGFP-cPLA₂α (green) were analyzed by confocal microscopy before (preadipocytes) and 8 days after adipogenic differentiation (adipocytes), as indicated. Nuclei were stained with DAPI (blue) and lipid droplets with Oil Red O (Red). (F) 3T3-L1 adipocytes transfected with EGFP-cPLA₂α (green) were immunostained with antibodies against p115 (red) and analyzed by confocal microscopy. Error bars represent the SEM of three independent determinations and statistical significance is indicated * p<0.05, ** p<0.01. The experiments shown are representative of at least three different ones.

FIGURE 6. *cPLA₂α affects mitotic clonal expansion during adipogenesis.* (A) 3T3-L1 cells were treated with siRNA control or against cPLA₂α and induced to differentiate. Quantification of viable cells was performed by the MTT assay and relative absorbance in each point over control cells at t=0 is shown. (B) Cells treated and induced as in A for 24 h were stained with PI and analyzed by flow cytometry. (C) Representation of percentage of cells in each phase of the cell cycle obtained from the analysis performed in B. (D) Homogenates from cells treated and induced as in A for the indicated periods of time were analyzed by immunoblot using antibodies against Cyclin A, Cdk2 and β-Actin. Relative quantification of specific bands against β-Actin is shown in lower panels. (E) Homogenates from cells treated and induced as in A for the indicated periods of time were analyzed by immunoblot using antibodies against C/EBPβ and β-Actin. Relative quantification of specific bands against β-Actin is shown in lower panel. Data are representative of three independent experiments done in triplicate, error bars represent the SEM and statistical significance is indicated ** p<0.01.

FIGURE 7. *Effect of preadipocyte treatment with AA in early adipogenic events.* Confluent 3T3-L1 were treated or not with 100 μM AA for two days. After removal of AA cells were induced to differentiate. (A) Quantification of viable cells was performed by the MTT assay of 3T3-L1 cells treated and differentiated for 1 and 2 days. (B) Flow cytometry analysis of 3T3-L1 cells treated and differentiated for 20 h and stained with PI. (C) Representation of the percentage of cells in each phase of the cell cycle quantified as in B. (D) Immunoblot analysis of homogenates from cells differentiated during different periods of time. Antibodies against Cyclin A, Cdk2 and β-Actin were used. Relative quantification of specific bands against β-Actin is shown in lower panels. (E) Homogenates from 3T3-L1 cells were analyzed by immunoblot using antibodies against C/EBPβ and β-Actin. Lower panel represent the densitometric quantification of protein bands shown. The experiments shown are representative of at least three different ones. Error bars represent the SEM and statistical significance is indicated * p<0.05, ** p<0.01.

FIGURE 8. *Effect of preadipocyte treatment with AA in late adipogenic events.* (A) Confluent 3T3-L1 were treated or not with 100 μ M AA for two days. After removal of AA cells were induced to differentiate in adipocytes for different periods of time (days) and were stained with Oil Red O. Pictures from cells and culture plates are shown. Right panel shows the quantification of Oil Red O staining. (B) Homogenates from 3T3-L1 cells treated and induced as in A were analyzed by immunoblot for the expression of the indicated proteins. At least three independent experiments were performed and a representative experiment is shown. (C) qPCR analysis of mRNA levels of the indicated genes were done in 3T3-L1 treated and differentiated as in A. (D) Homogenates from 3T3-L1 cells treated and differentiated as in A were analyzed by immunoblot using specific antibodies against cPLA₂α or β -Actin as a loading control. Relative densitometric quantification against β -Actin is shown in lower panel. (E) Confluent 3T3-L1 were treated or not with 100 μ M AA for two days in the presence of 50 μ M Indomethacin or the vehicle. Cells were then differentiated to adipocytes (8 days) and stained with Oil Red O. Pictures from culture plates are shown. Right panel shows the quantification of Oil Red O staining. Three independent experiments were done in triplicate. Error bars represent the SEM and statistical significance is indicated * $p < 0.05$, ** $p < 0.01$.

FIGURE 9. *cPLA₂α^{-/-} mice are protected against obesity induced by HFD.* (A) Homogenates from gonadal adipose tissue from cPLA₂α^{+/+} and cPLA₂α^{-/-} mice were analyzed by immunoblot using specific antibodies against cPLA₂α and β -Actin as a loading control. (B) A picture is shown of cPLA₂α^{+/+} and cPLA₂α^{-/-} mice after 16 weeks in a HFD. (C) cPLA₂α^{+/+} and cPLA₂α^{-/-} mice were weighted weekly during 16 weeks in a HFD or a normal diet. Mean body weights are represented (n=4). (D-J) Animals were fed a HFD for 16 weeks. (D) Weights of white (WAT) and brown adipose tissue (BAT) are represented normalized by body weight (n=4). (E) Lean mass is represented (n=4). (F) Micrographs of hematoxylin and eosin-stained sections of gonadal adipose tissue. Representative pictures are shown.. (G) Frequency distribution of adipocyte cell surface area. 1400 adipocytes from each genotype were analyzed (n=4). Statistical significant difference between the two groups was $p = 0.005$. (H) Calculated number of adipocytes in WAT is represented n=4. (I) Lipids from gonadal adipose tissue from animals were analyzed by mass-spectrometry. Mean quantifications for total triglycerides, cholesterol esters and phospholipids is shown. (n=4) (J) Analysis by qPCR of the mRNA levels of the indicated genes was performed in samples from gonadal adipose tissue from animals (n=4). Two independent experiments were done. Error bars represent the SEM and statistical significance is indicated * $p < 0.05$, ** $p < 0.01$, *** $p < 0.001$.

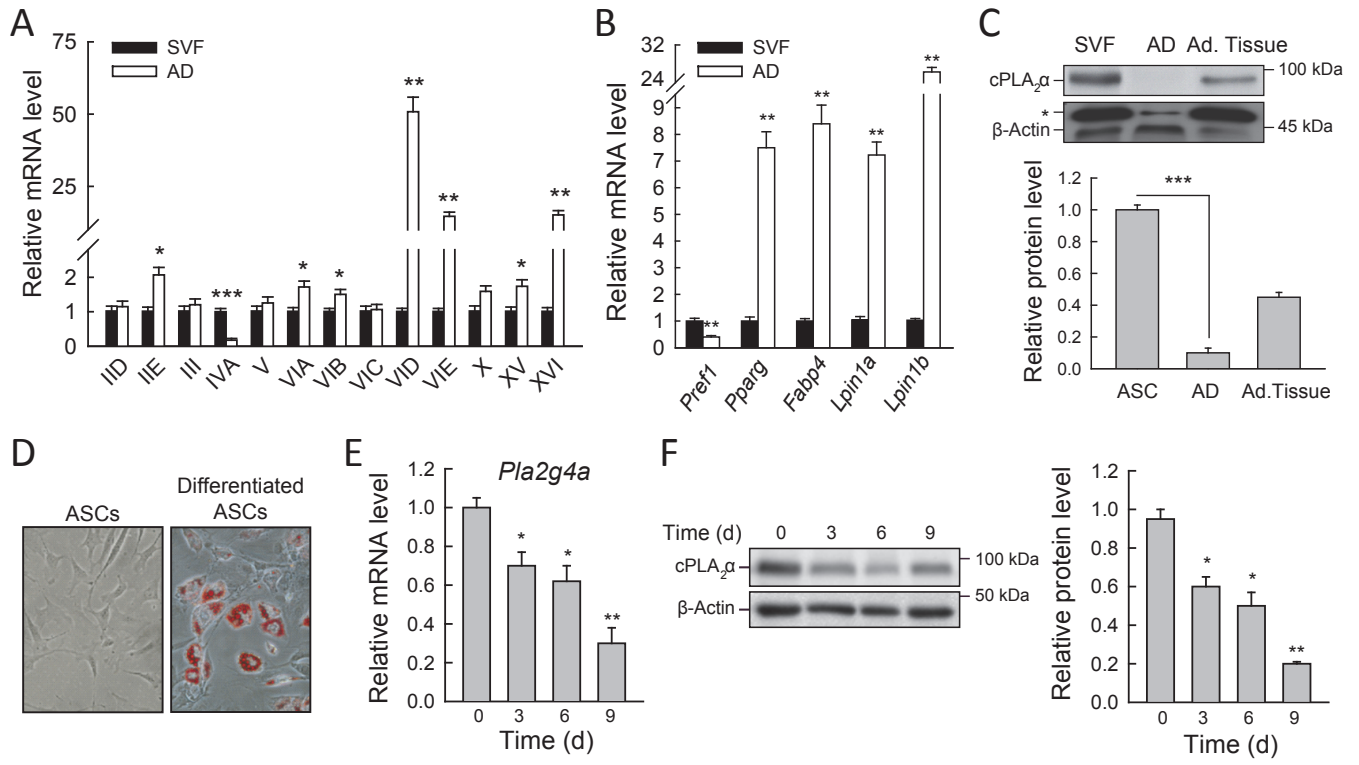


Figure 1

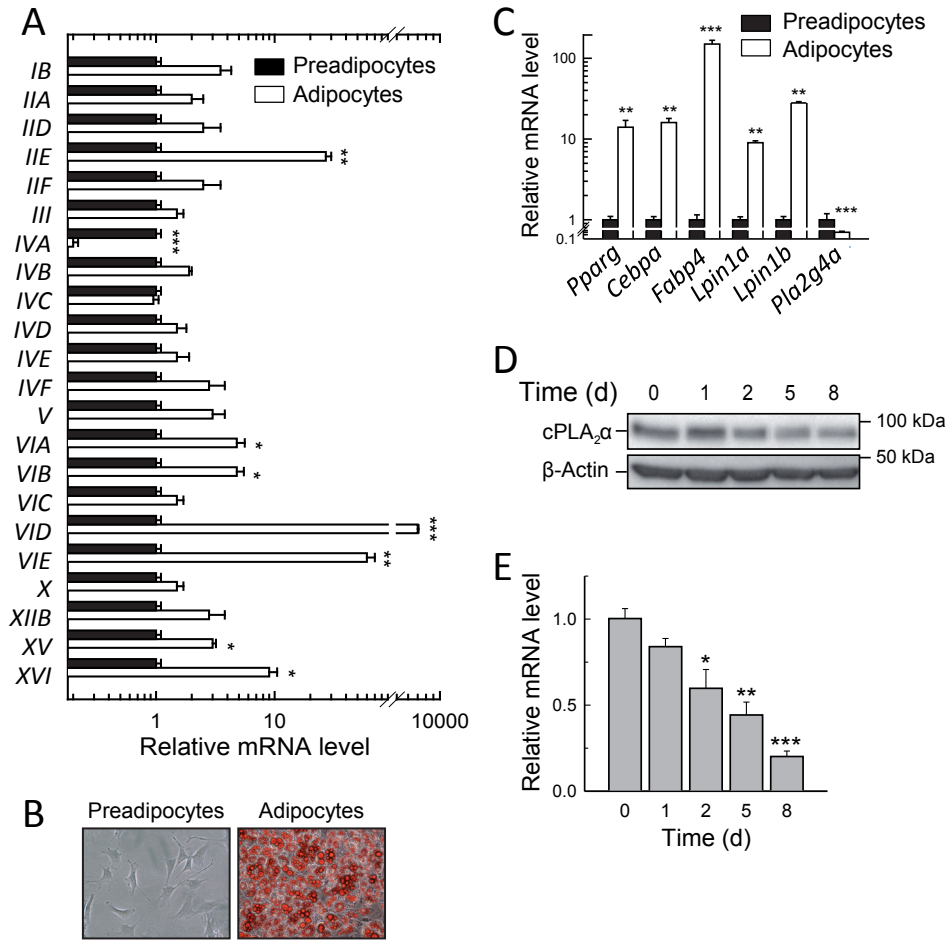
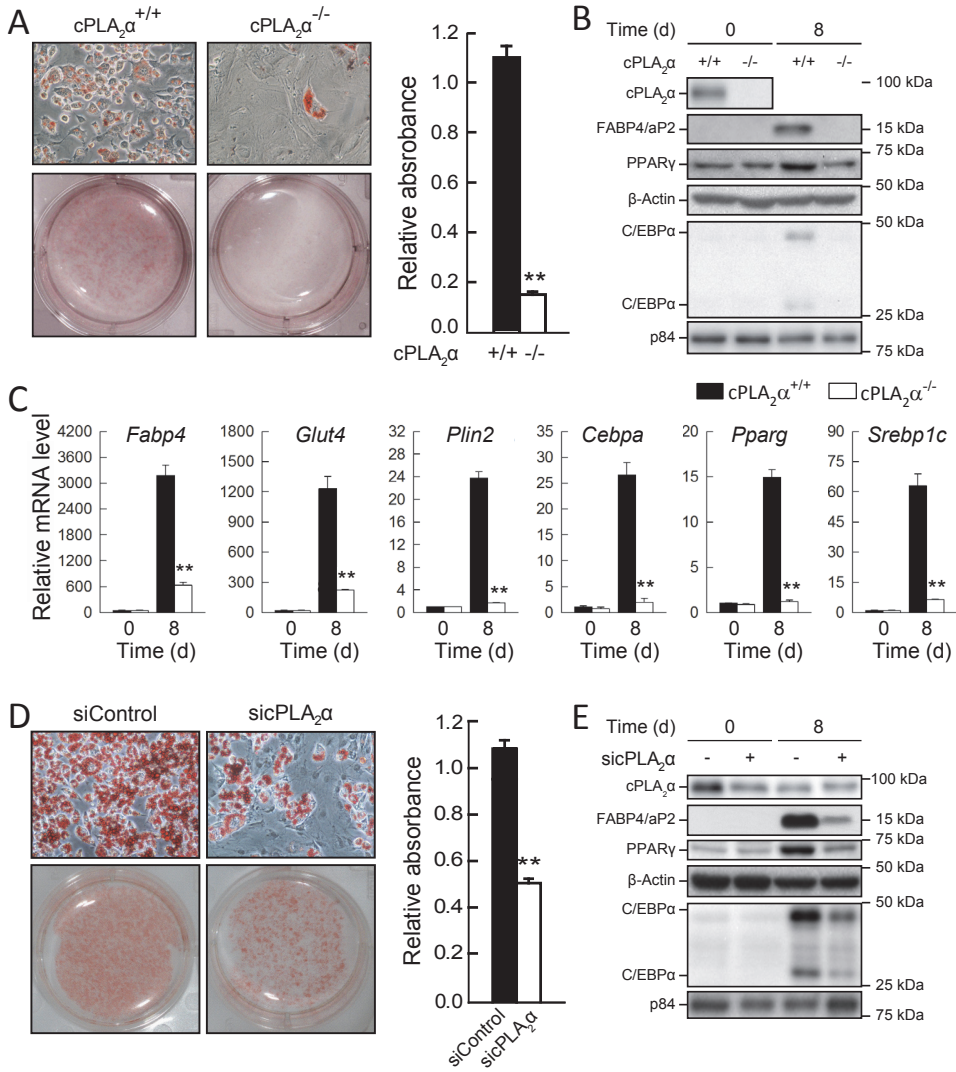


Figure 2



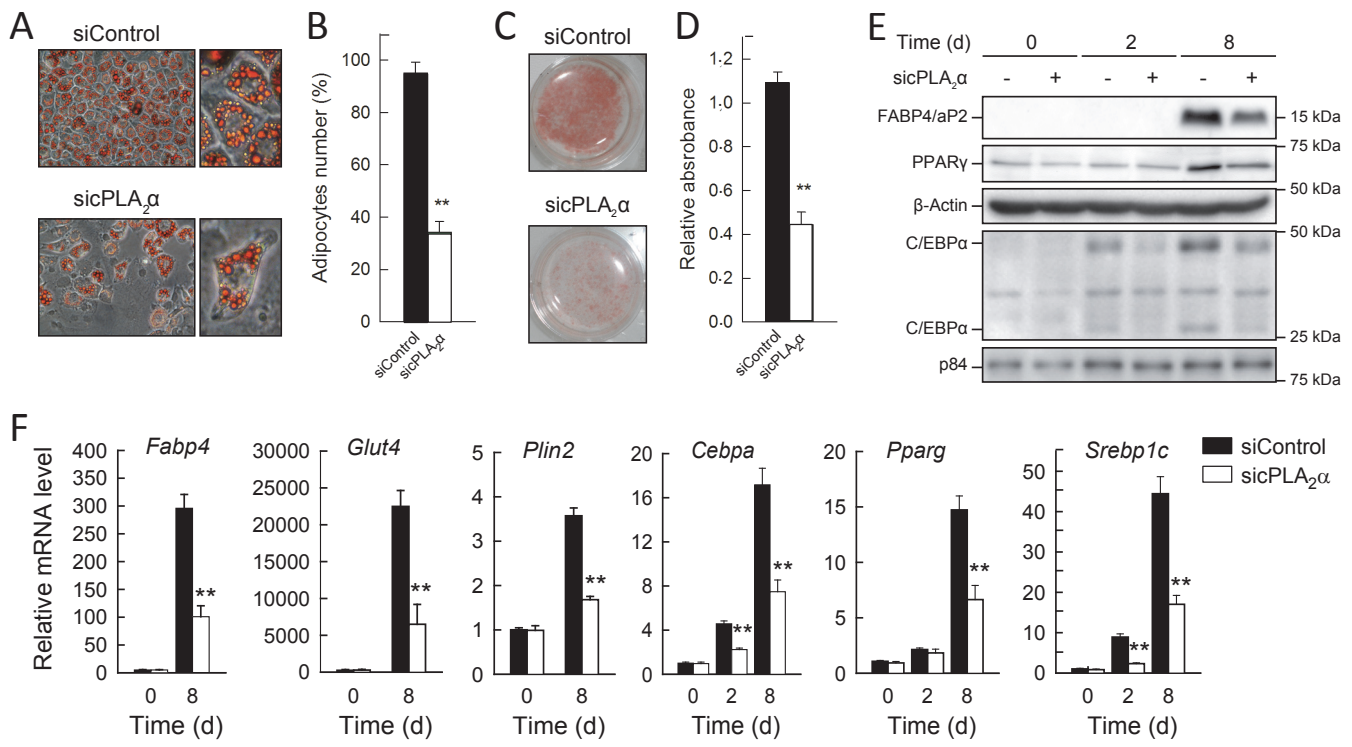


Figure 4

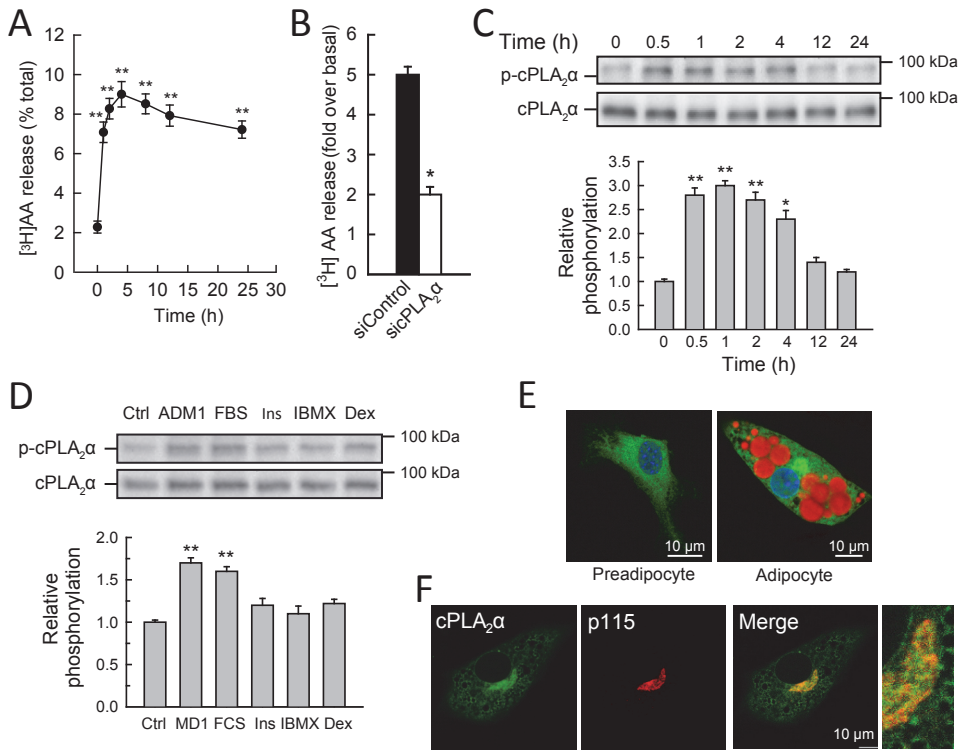


Figure 5

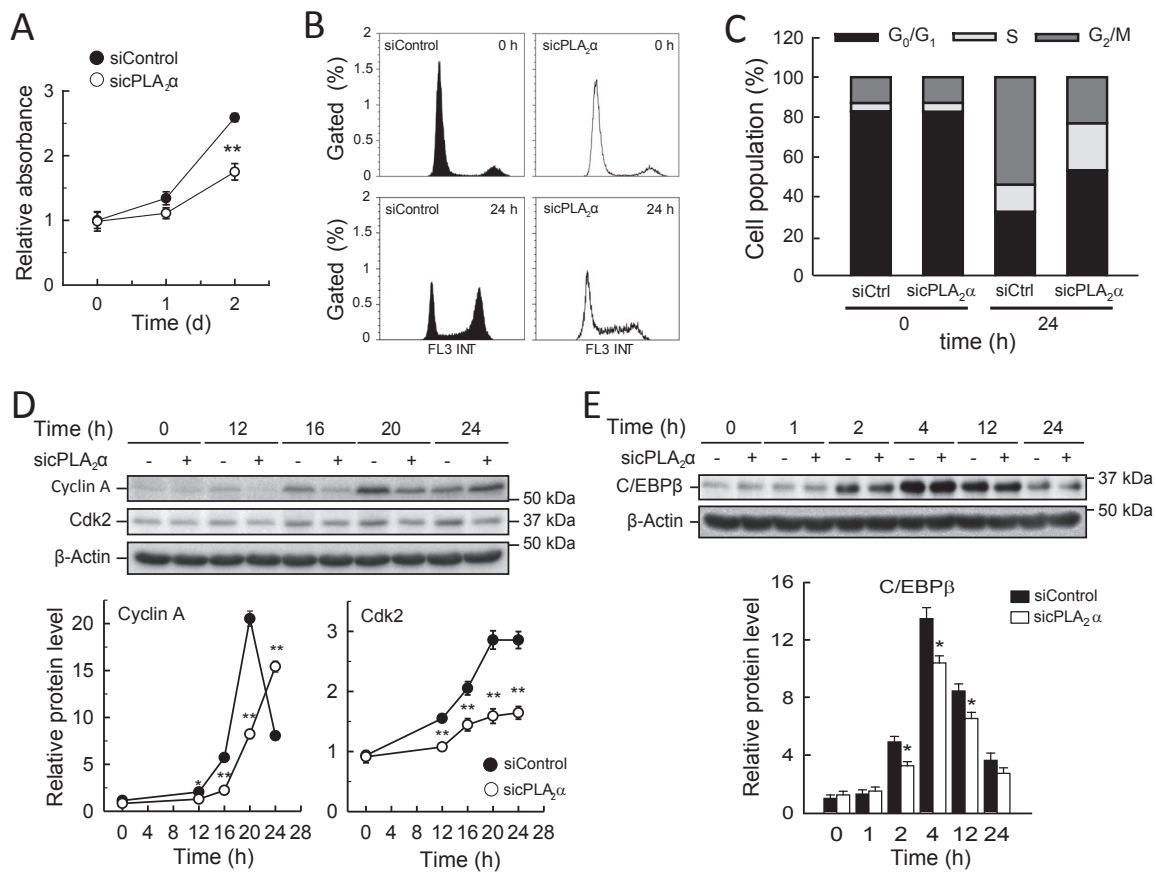


Figure 6

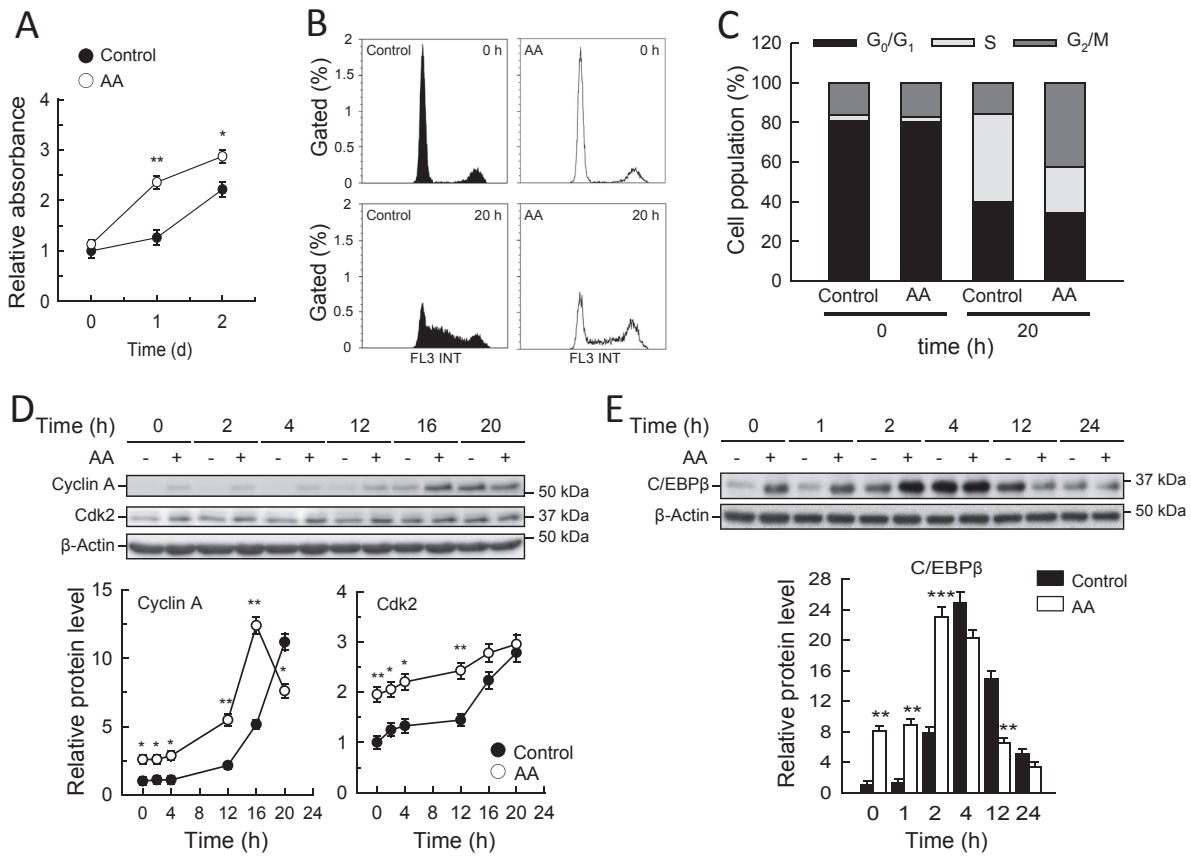


Figure 7

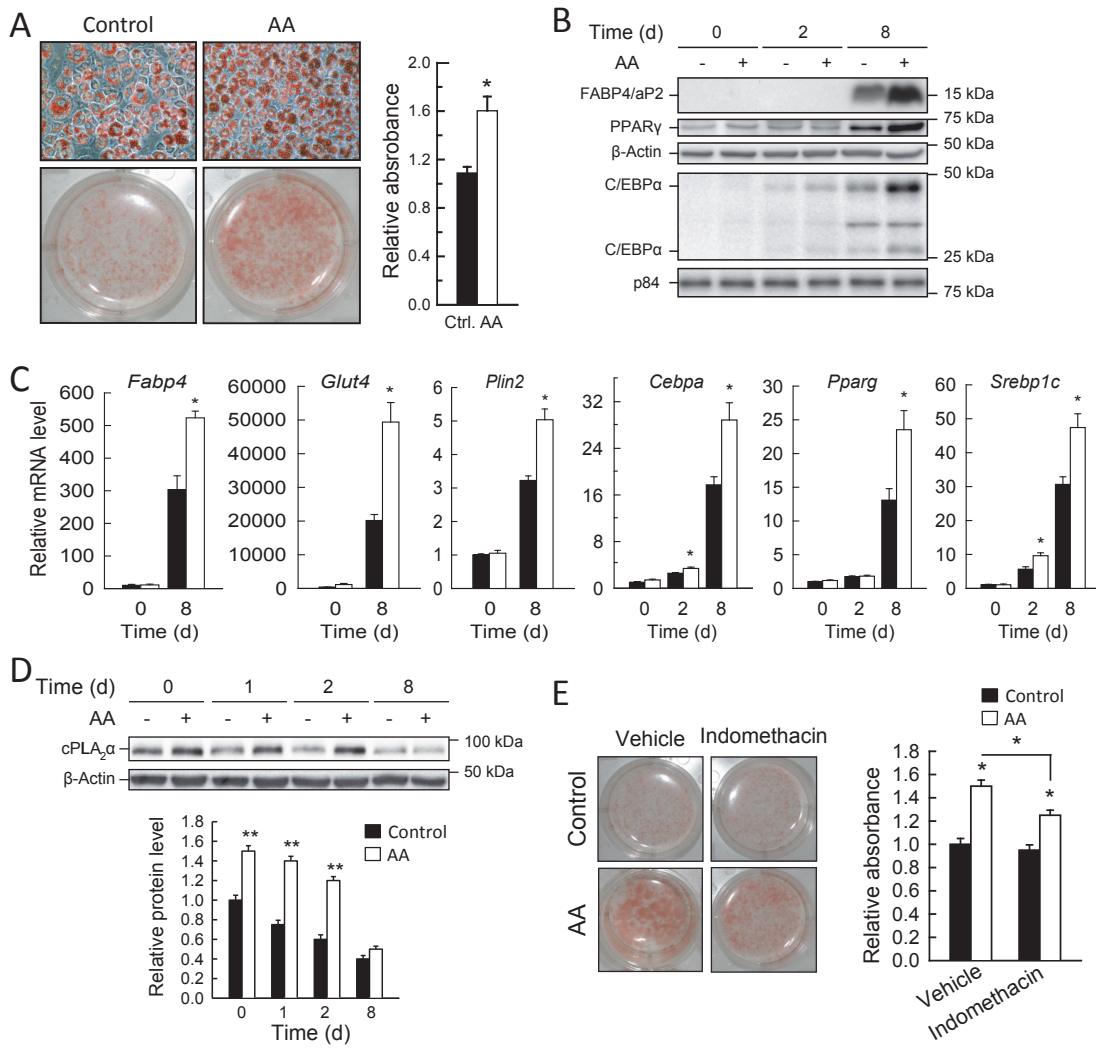


Figure 8

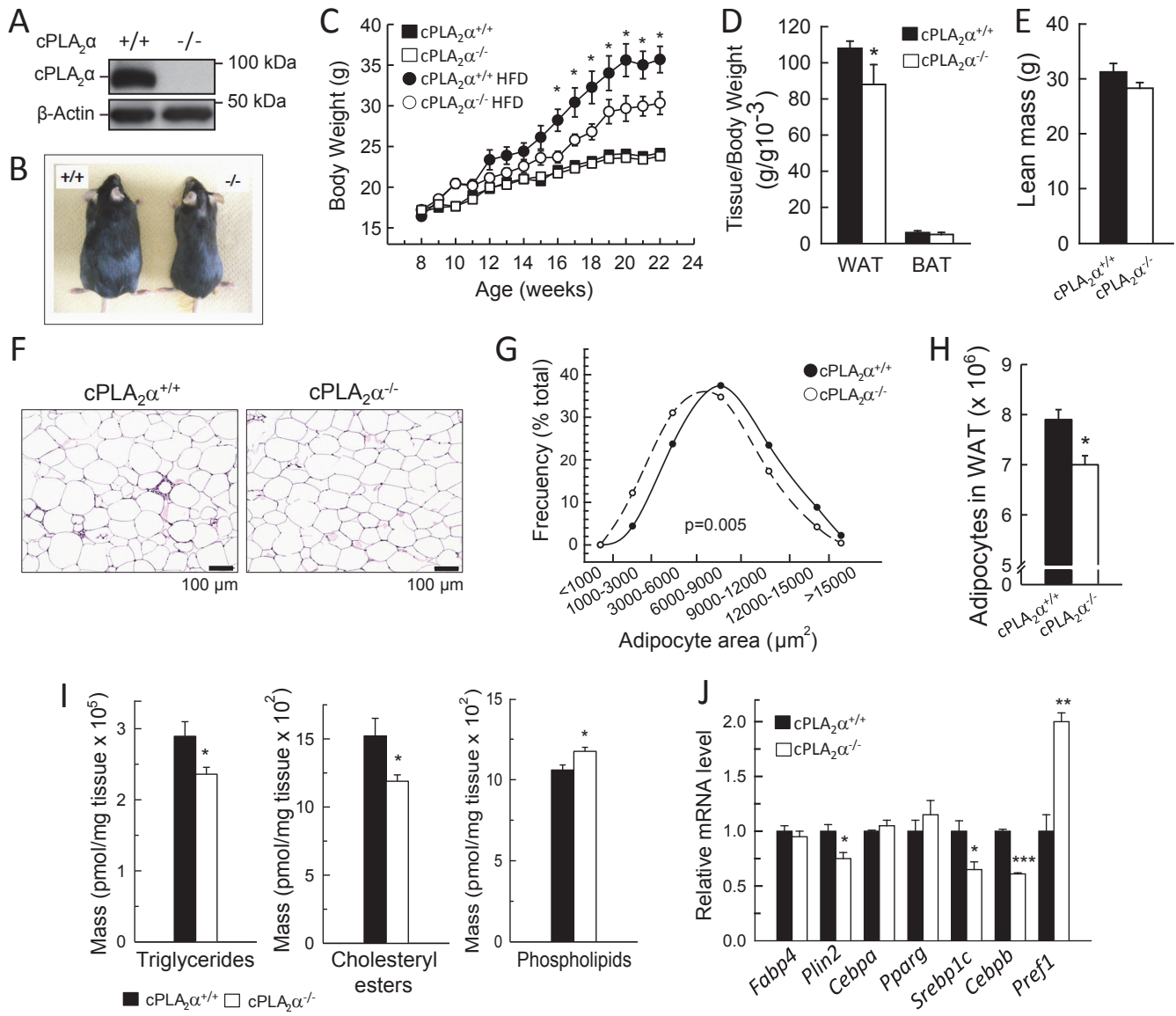


Figure 9